ChemComm

COMMUNICATION

View Article Online
View Journal | View Issue

Check for updates

Cite this: *Chem. Commun.*, 2025, **61**, 11421

Received 1st May 2025,
Accepted 18th June 2025

DOI: 10.1039/d5cc02409a

rsc.li/chemcomm

Open Access Article. Published on 18 June 2025. Downloaded on 2/16/2026 9:13:19 PM.
This article is licensed under a Creative Commons Attribution 3.0 Unported Licence.

Highly active iron catalysts for olefin hydrogenation enable *para*-hydrogen induced hyperpolarisation of ^{1}H and ^{19}F NMR resonances at 1.4 Tesla†

Julianna S. Doll,‡[a] Jan Kergassner,‡[b] Bingyu Zhang,[b] Christina M. Thiele,[c] Gerd Buntkowsky,[b] Markus Enders,[a] Torsten Gutmann*[b] and Dragoş-Adrian Roşca*[ad]

***para*-Hydrogen induced polarisation (PHIP) is an excellent tool for extracting mechanistic information in catalysis since it circumvents the intrinsic low sensitivity of nuclear magnetic resonance (NMR) spectroscopy. We report a class of iron complexes that are highly active in olefin hydrogenation catalysis and act as PHIP catalysts at 1.4 Tesla. Moreover, hyperpolarisation transfer to ^{19}F is observed.**

para-Hydrogen induced polarisation (PHIP) represents a powerful mechanistic tool, which enables the use of NMR spectroscopy to obtain local chemical environment information through a boost in sensitivity by several orders of magnitude.[1] Within the field of PHIP, special approaches such as the hydrogenation of the side arm (PHIP-SAH) have been established to broaden the variety of accessible substrate systems and to optimise signal enhancement.[2] The PHIP approach is currently used successfully in catalysis[3] and biomolecular NMR,[4] and relies on magnetic hyperpolarisation, usually through the incorporation of *para*-hydrogen (p-H_2) in an organic substrate, through catalytic hydrogenation. In homogeneous catalysis, PHIP has enabled the detection of very low concentrations of metal-based intermediates under catalytic conditions, which would have been impossible to detect otherwise by NMR spectroscopy.[5] Currently, PHIP catalysts based on noble metals (*i.e.* Rh, Ir, Pd, and Pt) dominate the field. Nevertheless, for the application of PHIP in bioimaging studies, reliance on noble metals has been seen as a hindrance to its implementation.[6]

In an effort to design catalysts based on more biocompatible and non-geopolitically geopolitically-source base metals, the last 20 years have seen rapid progress in the development of earth-abundant systems that exhibit hydrogenation activities comparable to those of noble metals. In iron chemistry, systems based on redox-active ligands are amongst the most active catalysts known for olefin functionalisation, such as hydroelementation or [2+2]-cycloaddition.[7] In the direct catalytic hydrogenation of olefins, such systems can promote turnover at loadings as low as 0.1 mol%,[8,9] which is comparable to and even surpasses the performance of established catalysts based on rhodium and iridium.[10]

This success, however, has not yet been mirrored in the development of PHIP catalysts based on iron. Unlike noble-metal catalysts, which typically operate *via* $2e^-$ redox steps, in the case of iron, $1e^-$ steps tend to be favourable. The resulting paramagnetic species involved are known to catalyse the conversion of p-H_2 back to the equilibrium mixture of *ortho*-hydrogen (o-H_2) and p-H_2 (a 75 : 25 ratio at RT).[11] Thus, until now, there have been very few examples employing iron-based catalysts for reactions involving p-H_2.[12] Recently, Fout *et al.* reported a rigid, redox-innocent pincer system based on two flanking NHCs as strong σ-donors and a phenyl ring, which can stabilize an iron hydride species (Fig. 1).[13] This system is an active catalyst for olefin hydrogenation (down to 1 mol% catalyst loading), and remarkably, PHIP of the hydrogenation products was observed. We herein report another family of iron-based PHIP catalysts based on a potentially redox-active ligand, capable of hydrogenating olefins at catalyst loadings as low as 0.1 mol%. In addition to the PHIP effect observed at 1.4 T on the ^{1}H resonances of the hydrogenated substate, transfer of polarisation to ^{19}F resonances is also observed. This opens an interesting pathway to iron-based PHIP catalysts capable of polarizing marker molecules with potential applications in MRI.[14] We have previously reported that the PNN-ligand (PNN = phosphine α-iminopyridine) framework can stabilise dinuclear iron dinitrogen complexes (**1**), as well as a rare example of an anionic iron hydride complex bearing a N_2 ligand (**2**).[15] While both complexes

[a] *Anorganisch-Chemisches Institut, Im Neuenheimer Feld 276, Universität Heidelberg, D-69120 Heidelberg, Germany. E-mail: dragos.rosca@uni-heidelberg.de, dragos-adrian.rosca@univ-rennes.fr*
[b] *Technische Universität Darmstadt, Eduard-Zintl-Institut für Anorganische und Physikalische Chemie, Peter-Grünberg-Straße 8, D-64287 Darmstadt, Germany. E-mail: gutmann@chemie.tu-darmstadt.de*
[c] *Technische Universität Darmstadt, Clemens-Schöpf-Institut für Organische Chemie und Biochemie, Peter-Grünberg-Straße 16, D-64287 Darmstadt, Germany*
[d] *Institut des Sciences Chimiques de Rennes, Université de Rennes, F-35000, Rennes, France*

† Electronic supplementary information (ESI) available. See DOI: https://doi.org/10.1039/d5cc02409a

‡ These authors contributed equally to this work.

Open Access Article. Published on 18 June 2025. Downloaded on 2/16/2026 9:13:19 PM.
This article is licensed under a Creative Commons Attribution 3.0 Unported Licence.

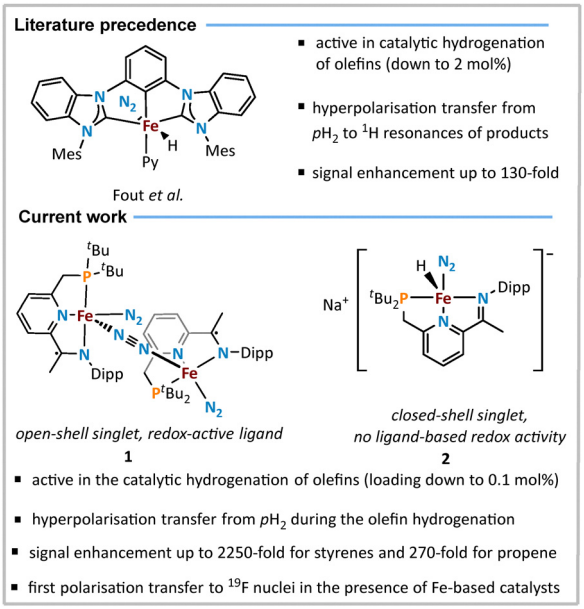

Fig. 1 State-of-the-art iron-based molecular PHIP catalysts.

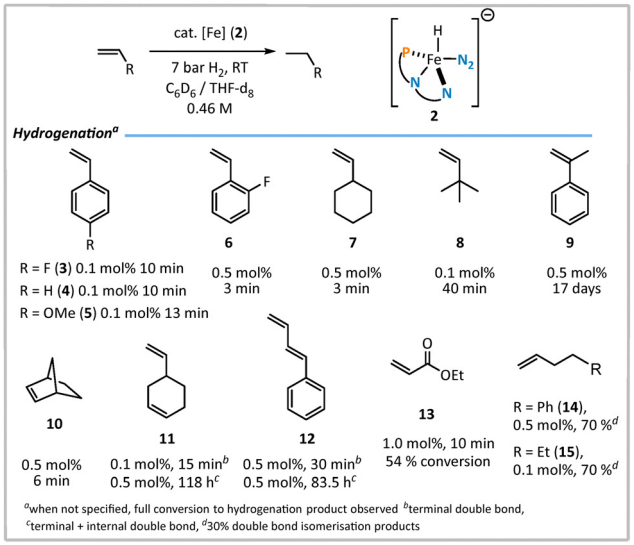

Fig. 2 Olefin hydrogenation substrate scope using **2** as a pre-catalyst. Conversions were determined by ^{1}H NMR spectroscopy with respect to an internal standard (C_6Me_6).

are based on formal Fe(0) centres, exhibiting a singlet ground state, the electronic structures of these complexes are significantly different. Namely, for $[PNNFe(N_2)]_2(\mu\text{-}N_2)$ (**1**), the PNN ligand is redox non-innocent with a narrow singlet–triplet separation (ΔE_{ST} = 3.7 kcal mol^{-1}, DFT), while **2** has a closed-shell singlet ground state, featuring a redox-inactive PNN chelate and a considerably widened singlet triplet separation (ΔE_{ST} = 9.2 kcal mol^{-1}, see the ESI†).[15]

Since **1** and **2** possess labile N_2 ligands, which can be displaced by more π-accepting olefins, they seem well-suited for olefin functionalisation reactions such as hydrogenation. Both systems are highly active in catalytic hydrogenation of olefins at low catalyst loadings (Fig. 2). Under the same reaction conditions (0.1 mol% loading per Fe centre, 7 bar H_2, RT) using *p*-F-styrene **3** as a model substrate, hydride **2** displayed slightly higher activity (full conversion in 10 min) when compared to **1** (97% conversion after 15 min). Hydride **2** can additionally hydrogenate a wide range of mono-substituted aromatic and aliphatic olefins (**3–8**). Geminal disubstituted olefins (**9**) remained reactive, albeit with a significantly lower reaction rate. Activated internal olefins (*e.g.* norbornene **10**) underwent hydrogenation rapidly, while less activated internal olefins (**11** and **12**) required significantly longer reaction times. Interestingly, conjugated olefins (*e.g.* **12**) did not resist turnover, suggesting that an η^4-diene intermediate is not a viable thermodynamic sink in this methodology. In the absence of H_2, styrene derivatives undergo polymerisation in the presence of **2** at higher catalyst loadings (>0.5 mol%) and higher substrate concentrations (>1.4 M), while this side reaction could mostly be suppressed at lower catalyst loadings and concentrations (<0.5 mol%, <0.7 M). An exception to this is *o*- and *m*-F-styrenes (*vide infra*). Substrates containing more fragile functional groups (*e.g.* esters, **15**) required higher catalyst loadings and led to incomplete conversion. For longer chain olefins (**14** and **15**), in addition to olefin hydrogenation, competitive double bond isomerisation was observed (*ca.* 30%). Vinylic phenols and allylic amines remained unreactive (see the ESI†).

Given the high activity of **1** and **2** in olefin hydrogenation, we investigated the catalytic conversion of styrene substrates in the presence of *para*-hydrogen (*p*-H_2). For polarisation transfer from *p*-H_2 to the hydrogenated substrate to occur, a series of pre-conditions are required, including (i) the pair-wise addition of H_2 to the substrate needs to occur with the breaking of symmetry of *p*-H_2, (ii) the transfer of hydrogen atoms to the substrate needs to proceed faster than the relaxation of the nuclear spin of the product,[16] and (iii) the formation of paramagnetic (or ferromagnetic) particles needs to be inhibited, as this can lead to a faster spin relaxation.

The fulfilment of pre-conditions (i) and (ii) mandates the hydrogenation of unsymmetrical olefinic substrates, mediated by highly active catalytic systems. We have chosen propene and *p*-F-styrene (**3**) as representatives of aliphatic and aromatic olefins as model substrates, in the presence of iron-based catalysts **1** and **2**. Since the two catalysts are structurally similar but have very different electronic structures (*vide supra*), subjecting the two systems to PHIP conditions would reveal more information about ligand design in iron-based polarisation transfer methodologies. Under ALTADENA conditions,[17] the hydrogenation of propene and *p*-F-styrene (**3**) was performed with catalyst **1** or **2**, respectively, by treatment with 4 bar *p*-H_2 and subsequent transfer of the appropriate sample into the probe of a 1.4 T benchtop NMR spectrometer. The signal enhancements (labelled as ε_1 for catalyst **1** and ε_2 for catalyst **2**) and decays of polarisation obtained in ^{1}H NMR were monitored in THF-d_8 and C_6D_6 solutions for **1**, and in only THF-d_8 solution for **2** due to solubility reasons. The obtained ^{1}H signal enhancement factors are summarized in Table S1 (ESI†) and the corresponding spectra are shown in Fig. S37–S45 (ESI†).

As shown in Fig. 3a, for propene, the highest ^{1}H enhancement of 270 was obtained with **1** in THF-d_8, while for *p*-F-styrene

 This journal is © The Royal Society of Chemistry 2025

Open Access Article. Published on 18 June 2025. Downloaded on 2/16/2026 9:13:19 PM.
This article is licensed under a Creative Commons Attribution 3.0 Unported Licence.

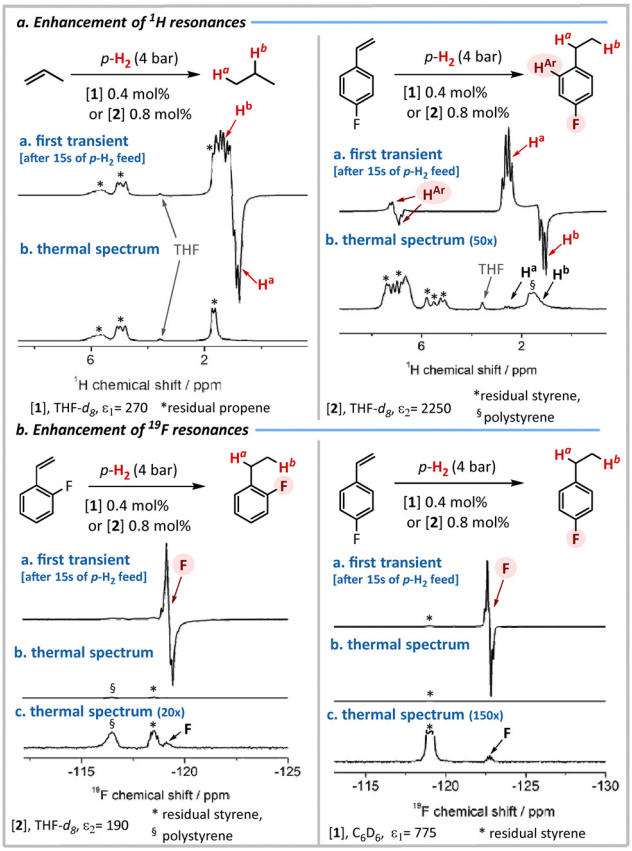

Fig. 3 A summary of the PHIP experiments and excerpts from ^{1}H (a) and ^{19}F (b) NMR data (RT, 1.4 Tesla benchtop NMR spectrometer). For the full dataset, see the ESI.†

(**3**) the highest enhancement of 2250 was obtained with **2** in THF-d_8, which corresponds to a polarisation of 1.09%, as described in the ESI.† In comparison, the enhancement reported in ref. 13 (*ca.* 200) corresponds to a polarisation of 0.97%, which is statistically identical. This convincingly demonstrates the feasibility of ^{1}H PHIP at 1.4 Tesla for both gaseous and liquid substrates employing catalysts **1** and **2** in THF-d_8. For the hydrogenation of **3** with catalyst **1**, the influence of solvent on the enhancement factor was investigated. An impact is observed (ε_1 = 415 for THF-d_8, ε_1 = 515 for C_6D_6), in line with previous reports on rhodium and iridium catalysts.[18] Since various parameters influence the obtained enhancement (see the ESI†), systematic studies are required, which are beyond the scope of this communication.

Subsequently, we have studied the feasibility of PHIP polarization transfer from ^{1}H to ^{19}F. To measure the dependence of the enhancement factor on the position of substitution, we have explored *o*-F-styrene (**6**) and *p*-F-styrene (**3**) as substrates under ALTADENA conditions.§ The ^{19}F signal enhancement factors are summarised in Table S1 (ESI†), and the corresponding spectra are shown in Fig. S46–S50 (ESI†). As illustrated in Fig. 3b, both catalysts **1** and **2** show PHIP transfer to ^{19}F, with enhancement factors of up to 190 obtained for *o*-F-styrene with catalyst **2** in THF-d_8. In C_6D_6, polarization transfer to ^{19}F with catalyst **1** is even more efficient, leading to an enhancement factor of 775 obtained for *p*-F-styrene. This again demonstrates the influence of the solvent on the signal enhancement. Comparison of enhancement factors for *o*- and *p*-fluoro substituents (30 *vs.* 95 for catalyst **1** and 190 *vs.* 200 for catalyst **2**) does not allow us to establish any clear trend with respect to the efficiency of polarization transfer as a function of styrene substitution. This is consistent with the results reported by Kuhn *et al.* who investigated ^{19}F PHIP polarization transfer for *o*- and *p*-F-styrenes with a Rh(I) catalyst.[14c] To the best of our knowledge, this is the first report of iron-mediated PHIP transfer to ^{19}F. It is interesting to note that PHIP can be observed with **1** despite the presence of the low-lying triplet states, the redox non-innocent nature of the chelating ligand and the absence of an Fe–H functional group (for the proposed mechanism, see the ESI†).

To gain further mechanistic insight into the catalytic hydrogenation, we investigated the reactivity of complex **2** toward styrenes and H_2 over a broader temperature range using NMR spectroscopy. Under H_2 pressure (7 bar, −40 °C to RT), **2** remained unchanged, although it readily formed the iron deuteride **2-d$_1$** with D_2, consistent with previous reports (see the ESI†). This selective reactivity, along with the observed PHIP in hydrogenation products, points towards the following mechanism (Fig. 4): (i) rapid formation of an η^2-olefin complex (**Int. 1**), especially in the presence of excess substrate; (ii) formation of a σ-H_2 complex (**Int. 3**) following the coordination of *para*-H_2 and (iii) selective transfer of the coordinated dihydrogen to the coordinated olefin to give rise to a hyperpolarised substrate. As a competing pathway, reversible olefin insertion into the Fe–H bond to give **Int. 2** is conceivable, but would probably not give rise to a hyperpolarised product. This pathway is also likely responsible for the observed styrene polymerisation reaction at higher catalyst loadings. Further mechanistic studies are required to determine to which extent the insertion pathway to give **Int. 2** is also involved in the productive catalytic hydrogenation pathway. Catalytic hydrogenation with D_2

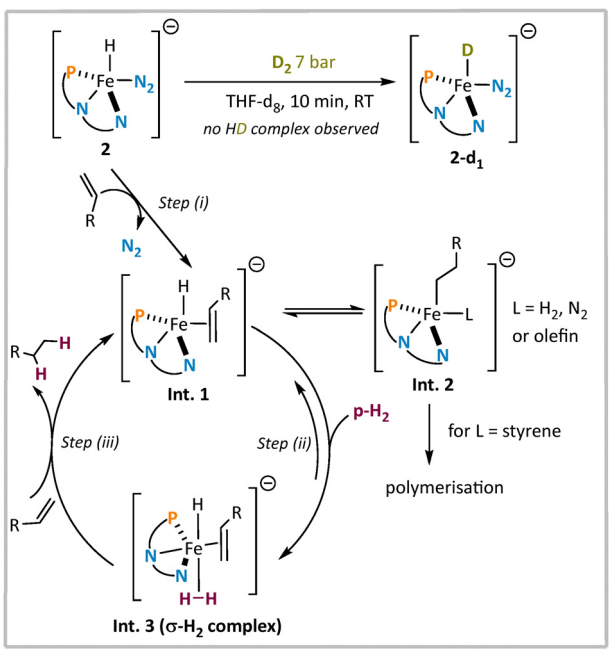

Fig. 4 Proposed mechanism for the hydrogenation of olefins in the presence of **2**.

Open Access Article. Published on 18 June 2025. Downloaded on 2/16/2026 9:13:19 PM.
This article is licensed under a Creative Commons Attribution 3.0 Unported Licence.

gives predominantly the 1,2-deuterated product, with minor amounts of terminal isotopomers (see the ESI†), suggesting reversible β-hydride elimination.

In conclusion, we have introduced two highly active iron catalysts, capable of hydrogenating aromatic and aliphatic olefins at loadings down to 0.1 mol%. Conducting the hydrogenation experiments on propene and *p*-F-styrene in the presence of *p*-H_2 allowed achieving enhancement factors of up to 270 and 2250, respectively, in THF-d_8 at 1.4 T (60 MHz benchtop spectrometer). We have also demonstrated for the first time that iron-based systems are capable of PHIP transfer to ^{19}F, with enhancement factors of up to 775 in C_6D_6 and up to 200 in THF-d_8 at 1.4 T. Interestingly, this work shows that in principle, both open-shell singlet iron complexes with low lying triplet states (**1**) and closed-shell iron complexes (**2**) can act as PHIP catalysts, demonstrating that ligand field strength is not the only parameter that governs the design of iron based PHIP catalysts. The current work lays the groundwork for a broader investigation of polarisation transfer to other heteronuclei using iron catalysis based on redox-active ligands, with the aim of replacing and complementing the established approaches based on noble metals (*e.g.* Rh and Ir).

This work was supported by the Deutsche Forschungsgemeinschaft (DFG grant RO5979/2-1 to D.-A. R.). J. K., B. Z., C. M. T., M. E., G. B. and T. G. thank the CRC 1487 "Iron Upgraded" funded by the DFG for financial support (project no. 443703006). Computational resources were provided by the state of Baden-Württemberg through bwHPC and the DFG (INST 40/575-1 FUGG, JUSTUS 2 cluster). The authors acknowledge Dr Eckhard Bill for measuring the Mössbauer spectrum of **2**. D.-A. R. is grateful to Prof. Lutz H. Gade for generous support over the years.

Conflicts of interest

There are no conflicts to declare.

Data availability

The data supporting this article, including experimental details and copies of the NMR spectra, have been included in the ESI.†

Notes and references

§ *m-F*-Styrene undergoes polymerisation under these reaction conditions and is not a suitable substrate for PHIP. See the ESI.†

1 (*a*) G. Buntkowsky, F. Theiss, J. Lins, Y. A. Miloslavina, L. Wienands, A. Kiryutin and A. Yurkovskaya, *RSC Adv.*, 2022, **12**, 12477–12506; (*b*) A. I. Silva Terra, D. A. Taylor and M. E. Halse, *Prog. Nucl. Magn. Reson. Spectrosc*, 2024, **144–145**, 153–178; (*c*) A. D. Robinson, F. Hill-Casey, S. B. Duckett and M. E. Halse, *Phys. Chem. Chem. Phys.*, 2024, **26**, 14317–14328; (*d*) T. Castaing-Cordier, D. Bouillaud, J. Farjon and P. Giraudeau, in *Annual Reports on NMR Spectroscopy*, ed. G. A. Webb, Academic Press, 2021, vol. 103, pp. 191–258; (*e*) F. Theiss, J. Lins, J. Kergassner, L. Wienands, S. Doller and G. Buntkowsky, *J. Magn. Reson.*, 2024, **362**, 107673.

2 (*a*) F. Reineri, T. Boi and S. Aime, *Nat. Commun.*, 2015, **6**, 5858; (*b*) O. G. Salnikov, N. V. Chukanov, A. N. Pravdivtsev, D. B. Burueva, S. V. Sviyazov, K. Them, J. B. Hovener and I. V. Koptyug, *ChemPhysChem*, 2025, e202401119.

3 (*a*) B. J. Tickner and V. V. Zhivonitko, *Chem. Sci.*, 2022, **13**, 4670–4696; (*b*) W. Wang, Q. Wang, J. Xu and F. Deng, *ACS Catal.*, 2023, **13**, 3501–3519; (*c*) S. B. Duckett and N. J. Wood, *Coord. Chem. Rev.*, 2008, **252**, 2278–2291; (*d*) A. N. Pravdivtsev, B. J. Tickner, S. Glöggler, J.-B. Hövener, G. Buntkowsky, S. B. Duckett, C. R. Bowers and V. V. Zhivonitko, *ACS Catal.*, 2025, **15**, 6386–6409; (*e*) T. C. Eisenschmid, R. U. Kirss, P. P. Deutsch, S. I. Hommeltoft, R. Eisenberg, J. Bargon, R. G. Lawler and A. L. Balch, *J. Am. Chem. Soc.*, 1987, **109**, 8089.

4 (*a*) F. Theiss, L. Wienands, J. Lins, M. Alcaraz-Janssen, C. M. Thiele and G. Buntkowsky, *Sci. Rep.*, 2023, **13**, 10117; (*b*) J. Lins, Y. A. Miloslavina, O. Avrutina, F. Theiss, S. Hofmann, H. Kolmar and G. Buntkowsky, *J. Am. Chem. Soc.*, 2024, **146**, 35175–35184.

5 (*a*) M. Leutzsch, L. M. Wolf, P. Gupta, M. Fuchs, W. Thiel, C. Fares and A. Fürstner, *Angew. Chem., Int. Ed.*, 2015, **54**, 12431–12436; (*b*) C. Godard, S. B. Duckett, S. Polas, R. Tooze and A. C. Whitwood, *J. Am. Chem. Soc.*, 2005, **127**, 4994–4995; (*c*) S. B. Duckett, C. L. Newell and R. Eisenberg, *J. Am. Chem. Soc.*, 1994, **116**, 10548–10556; (*d*) A. Manoharan, P. J. Rayner, W. Iali, M. J. Burns, V. H. Perry and S. B. Duckett, *ChemMedChem*, 2018, **13**, 352–359.

6 A. Manoharan, P. J. Rayner, W. Iali, M. J. Burns, V. H. Perry and S. B. Duckett, *ChemMedChem*, 2018, **13**, 352–359.

7 (*a*) M. V. Joannou, J. M. Hoyt and P. J. Chirik, *J. Am. Chem. Soc.*, 2020, **142**, 5314–5330; (*b*) L. E. Hertwig, T. Bender, F. J. Becker, P. Jäger, S. Demeshko, S. J. Gross, J. Ballmann and D.-A. Roşca, *ACS Catal.*, 2023, **13**, 6416–6429.

8 (*a*) S. C. Bart, E. Lobkovsky and P. J. Chirik, *J. Am. Chem. Soc.*, 2004, **126**, 13794–13807; (*b*) A. Archer, M. W. Bouwkamp, M.-P. Cortez, E. Lobkovsky and P. J. Chirik, *Organometallics*, 2006, **25**, 4269–4278; (*c*) R. J. Trovitch, E. Lobkovsky, E. Bill and P. J. Chirik, *Organometallics*, 2008, 1470–1478; (*d*) R. P. Yu, J. M. Darmon, J. M. Hoyt, G. W. Margulieux, Z. R. Turner and P. J. Chirik, *ACS Catal.*, 2012, **2**, 1760–1764; (*e*) J. C. Ott, C. K. Blasius, H. Wadepohl and L. H. Gade, *Inorg. Chem.*, 2018, **57**, 3183–3191; (*f*) Y. Sunada, H. Ogushi, T. Yamamoto, S. Uto, M. Sawano, A. Tahara, H. Tanaka, Y. Shiota, K. Yoshizawa and H. Nagashima, *J. Am. Chem. Soc.*, 2018, **140**, 4119–4134.

9 (*a*) L. González-Sebastián, A. Reyes-Sanchez and D. Morales-Morales, *Organometallics*, 2023, **42**, 2426–2446; (*b*) D. Wei and C. Darcel, *Chem. Rev.*, 2019, **119**, 2550–2610; (*c*) L. Alig, M. Fritz and S. Schneider, *Chem. Rev.*, 2019, **119**, 2681–2751.

10 H. U. Blaser, F. Spindler and M. Thommen, in *The Handbook of Homogeneous Hydrogenation*, ed. J. G. de Vries, C. J. Elsevier, Wiley-VCH: Weinheim, 2008, Ch. 37, pp. 1279–1324.

11 (*a*) L. Yang, X. Li, Y. Chen, X. Zheng and K. Sun, *Sci. Rep.*, 2024, **14**, 20925; (*b*) T. Das, S.-C. Kweon, I. W. Nah, S. W. Karng, J.-G. Choi and I.-H. Oh, *Cryogenics*, 2015, **69**, 36–43.

12 (*a*) A. M. Balu, S. B. Duckett and R. Luque, *Dalton Trans.*, 2009, 5074; (*b*) L. Kaltschnee, A. N. Pravdivtsev, M. Gehl, G. Huang, G. L. Stoychev, C. Riplinger, M. Keitel, F. Neese, J.-B. Hövener, A. A. Auer, C. Griesinger, S. Shima and S. Glöggler, *Nat. Catal.*, 2024, **7**, 1417–1429; (*c*) D. Schott, P. Callaghan, J. Dunne, S. B. Duckett, C. Godard, J. M. Goicoechea, J. N. Harvey, J. P. Lowe, R. J. Mawby, G. Müller, R. N. Perutz, R. Poli and M. K. Whittlesey, *Dalton Trans.*, 2004, 3218.

13 D. C. Najera and A. R. Fout, *J. Am. Chem. Soc.*, 2023, **145**, 21086.

14 (*a*) U. Bommerich, T. Trantzschel, S. Mulla-Osman, G. Buntkowsky, J. Bargon and J. Bernarding, *Phys. Chem. Chem. Phys.*, 2010, **12**, 10309–10312; (*b*) M. Plaumann, U. Bommerich, T. Trantzschel, D. Lego, S. Dillenberger, G. Sauer, J. Bargon, G. Buntkowsky and J. Bernarding, *Chem. – Eur. J.*, 2013, **19**, 6334–6339; (*c*) L. T. Kuhn, U. Bommerich and J. Bargon, *J. Phys. Chem. A*, 2006, **110**, 3521–3526; (*d*) A. S. Kiryutin, K. L. Ivanov, A. V. Yurkovskaya, R. Kaptein and H.-M. Vieth, *Z. Phys. Chem.*, 2012, **226**, 1343–1362.

15 (*a*) N. I. Regenauer, H. Wadepohl and D.-A. Roşca, *Inorg. Chem.*, 2022, **61**, 7426–7435; (*b*) N. I. Regenauer, H. Wadepohl and D. A. Roşca, *Chem. – Eur. J.*, 2022, e202202172.

16 S. B. Duckett and R. E. Mewis, *Acc. Chem. Res.*, 2012, **45**, 1247–1257.

17 J. Eills, D. Budker, S. Cavagnero, E. Y. Chekmenev, S. J. Elliott, S. Jannin, A. Lesage, J. Matysik, T. Meersmann, T. Prisner, J. A. Reimer, H. Yang and I. V. Koptyug, *Chem. Rev.*, 2023, **123**, 1417–1551.

18 (*a*) O. Bondar, E. Cavallari, C. Carrera, S. Aime and F. Reineri, *Catal. Today*, 2022, **397–399**, 94–102; (*b*) T. Gutmann, T. Ratajczyk, S. Dillenberger, Y. Xu, A. Grünberg, H. Breitzke, U. Bommerich, T. Trantzschel, J. Bernarding and G. Buntkowsky, *Solid State Nucl. Magn. Reson.*, 2011, **40**, 88–90.

This journal is © The Royal Society of Chemistry 2025